Arabian Journal for Science and Engineering
https://doi.org/10.1007/s13369-021-06092-7

RESEARCH ARTICLE-MECHANICAL ENGINEERING

EMHD Flow of Radiative Second-Grade Nanofluid over a Riga Plate due to Convective Heating: Revised Buongiorno's Nanofluid Model

Kotha Gangadhar[1] · **Manda Aruna Kumari**[1] · **Ali J. Chamkha**[2]

Received: 2 June 2021 / Accepted: 13 August 2021

Abstract

Exploiting the impact of Lorentz force and convective heating boundary on second-grade nanofluid flow alongside a Riga pattern is the main objective of the present work. Modelling of the present work is done through Grinberg term and a Lorentz force applied parallel to the wall of a Riga plate. The nanoparticles fraction on the solid surface of Riga pattern maintained a strong retardation because of zero mass flux. Theories of Cattaneo–Christov heat flux and generalized Fick's relations are employed by following the modern aspects of heat and mass transportations. In the current study, additional features of thermal radiation are also included in the energy equation in terms of linear expressions. In order to make the analysis more worthy, effect of chemical reaction is also included. By applying the suitable variables, constituted problem is converted into dimensionless form. Solution of the problem with desired accuracy is obtained by utilizing popular method called Runge–Kutta–Fehlberg. The graphical representations are used to illustrate the flow controlling parameters involved by their attractive physical consequences. Velocity distribution is observed for the increase with the second-grade parameter. Further, an improved nanoparticles temperature distribution is observed with the increase in radiation parameter and Biot number. Additionally, the distribution of the concentration of nanoparticles increases with increase in values of the thermophoretic parameter. Based on the scientific calculations obtained, it is established that the reported results may play a useful role in production processes and in the improvement of energy and thermal resources.

Keywords Thermal radiation · Riga plate · Modified second-grade nanofluid · Zero mass flux · Cattaneo–Christov heat flux

1 Introduction

From the recent days, the development era of nanodevices involves focusing on the nanotechnology-based fluid flow which has been played as an important role. Heat transfer in base fluid is introduced by the nanofluids which become to create a new era in the engineering and technology field at the same time. It is for sure needed to improve the heat transfer characteristics for the effectiveness improvement of several processes along with the use of some new agents. Particles with nanometer size called as nanoparticles are therefore responsible in heat transfer improvement. So these nanofluids find various applications in industry such as micro-channel heat lubricants and sinks, heat exchangers, coolants and anticancer therapy. Likewise, in late decades, several examiners have been occupied with considering nanofluids applications in different fields. For example, the idea of nanofluids was built by the Choi [1] on advances in cooling. Normal fluids such as ethylene glycol, oil and water inherently have low thermal conductivity, which limits the ability to transfer heat. Further advancement of heat transfer is required by saving vitality due to the development of innovations through the downsizing of electronic devices. The elegance of a new fluid is resulted by tackling such challenging situation called a nanofluid. Nanofluid has a high potential for improving the rate of heat transfer in building structures, especially for cooling electronic devices because thermal conductivity of nanofluid is higher compared to the

✉ Ali J. Chamkha
a.chamkha@kcst.edu.kw

Kotha Gangadhar
kgangadharmaths@gmail.com

Manda Aruna Kumari
arunakumaridarsanapu@gmail.com

[1] Department of Mathematics, Acharya Nagarjuna University Campus, Ongole, Andhra Pradesh 523001, India

[2] Faculty of Engineering, Kuwait College of Science and Engineering, Doha District, Kuwait

Published online: 28 August 2021

normal fluids. In this point of view, Beiki [2] studied convective mass transfer of nanofluids in a circular tube.

Buongiorno [3] showed that if the single-phase model is used in heat transfer coefficient of the nanofluid prediction then it contradicts experimental perception and unadulterated fluid relations (e.g. Dittus-Boelter). At that time, an alternative model was created that eliminated the shortcomings of single-phase/scattering (discrete phase models). He thought of seven gliding tools when he hypothesized that unique thermophoresis and Brownian diffusion were the overwhelming gliding instruments in nanoliquids. Based on these results, then the non-homogeneous two-phase equilibrium model is proposed in nanoliquids for convective transport. Representing the influence of relative velocity between the nanoparticles and the base liquid more mechanically when contrasted to the scattering models is one of the advantages of this new model. Because of vertical plate, the convective boundary layer flow processed in the nanofluids is illustrated by the Kuznetsov and Nield [4]. Daniel et al. [5] discussed nanofluid flow and slip mechanism over a stretched sheet. So many contributions of works are made in this direction in the past recent years [6–19].

Recently, priceless attempts have been performed for the flow of non-Newtonian because of their incomparable significance in chemical and processing industries, geophysics, materials processing and nuclear engineering, invaluable attempts have been made for them in recent times. Due to the interdisciplinary character of the non-Newtonian fluids, investigation on them has been an interesting research field in recent time. Most commonly, several chemical and processing industries have been using these fluids. It is needed to concentrate deeply on the significant factor that determines the rheology of these fluids by the mathematicians, physicists and engineers since that factor is very complex. These complex properties because of the nonlinear behaviour are addressed by a variety of fluid models that have been diversified by the several scientists. The differential type, integral type and velocity type are the three non-Newtonian fluids that were characterized into. The non-Newtonian model that determines the properties of normal stresses among those nonlinear models is categorized as second degree fluid. Rivlin and Ericksen and [20] were imposed the original basic tonsorial relations of that model in 1955. The constant viscosity attained by the second degree fluid model is often observed that it was not be interpreted for fluid models with relatively high viscosity. In view of these others related works [21–27].

It is well-acknowledged fact that electromagnetic forces are very helpful to control the flow of electric conducting fluids as well as with other classical methods, i.e. wall motion, suction and blowing. Electromagnetic force has the ability to atone the prescribed momentum deficit by activating a boundary layer. The propagation of strong electrically conducting materials, i.e. semi-conductor melts and liquid materials $\sigma \sim 106\,\mathrm{S/m}$, has been affected by extrinsic magnetic fields of balanced strengths about $\sim 1T$. Such kind of flow is called "Classical Magneto hydrodynamic Flow" control. However, in weakly electrically conducting materials [seawater $\sigma \sim 1 \times 10\,\mathrm{S/m}$], the amount of induced current due to an external magnetic field is very small, and hence, an external field is necessary to obtain the effective flow control. Such type of flow is known as electromagnet hydrodynamic flow control. The pressure gradient formed by boundary layer flow is affected by wall-parallel Lorentz force which is produced due to the cross-wise magnetic and electric field. This is also helpful to stabilize its propagation by decreasing its growth.

The wall-parallel Lorentz was created by an effective and efficient method which was introduced by the Lielausis and Gailitis in [28]. Like span-wise aligned arrays, permanent electrodes and magnets are designed with the inclusion of electromagnetic actuator which is introduced by them [see Fig. 1]. This geometry type can be identified as the Riga plate [29]. The process of turbulence production reducing and boundary layer separation prevention can be used to decrease the friction force and pressure drag of submarines. Then after this by using the Riga plates, Blasius flow improved stability is used the wall-parallel Lorentz force can be examined by Tsinober and Shtern [30]. Lorentz force boundary layer flow calculations use the Grinberg term [31] by Tsinober and Shtern [30]. Decoupling in the momentum expression of boundary layer by using this Grinberg term, it is independent on the stream velocity and it is reducing via y. A Riga plate is developed by Pantokratoras and Magyari [32], in which the permanent magnets and electrodes are altered in the alignment array of span-wise in 2009. According to Riga plate, viscous nanofluid flow is described by the Ahmed et al. [33]. By using the horizontal Riga plates, nanofluid EMHD slip features are mathematically calculated

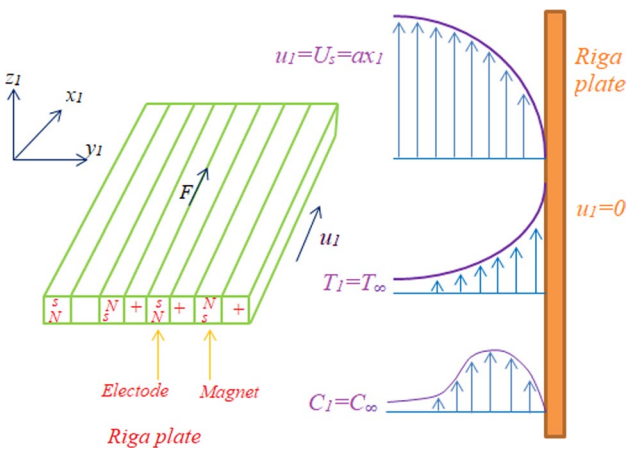

Fig. 1 Geometrical sketch

by the Ayub et al. [34]. EMHD recent methods are described in [35–41].

The information about EMHD and stretching sheets is fond easily in the literature, but Riga plate information in the fields of boundary layer formulations and mass and heat transport mechanism studies are limited in the literature. Chemical and thermal reactions in the Riga plate of second-grade nanofluid flow are affected by the Cattaneo–Christov model. An incompressible second-grade viscous nanofluid movement is considered along a convectively heated vertical Riga plate. Through the Grinberg term, Lorentz force is involved. By using suitably adjusted transformations, the nonlinear problems are converted into general differential equations. Nonlinear problems are finding their solutions by implementing the method of RKF-45. By the graphical illustrations, permanent parameters influenced on the fluid flow are explained. In the industrial applications, local Nusselt number and wall drag coefficient expressions are highly interested. These expressions are described.

2 Mathematical Formulation

The Riga plate placed at $y = 0$ considers electromagnet hydrodynamic (EMHD) flow of viscous incompressible second-grade nanofluid generated by the Riga plate subject to thermal radiation and chemical reaction. Flow is generated by the Riga plate which is located at $y = 0$ [see Fig. 1]. On a plane sheet, electrodes and magnets are placed and these are dividing from the different arrays of Riga plate. Lorentz forces are generated from the magnets of span-wise arrangements. According to constant heat fluid, the initial temperature $T = T_f$ is assumed with the opposite side plate of the model. Apart from surface of Riga pattern, at larger distance C_∞, ambient nanoparticles and T_∞ is the ambient thermal state concentration. $u = ax$ is free stream velocity in which a is a positive factor. A disclosed of aiding flow and mixed convective opposing. At thermal level, convective boundary condition is influenced and wall of the plate uses the zero mass flux condition.

The following expressions are satisfied by Cattaneo–Christov model (Rasool and Wakif [42]):

For energy,

$$\mathbf{p} + \lambda_p \left[(\nabla \mathbf{p}).\tilde{v} - (\nabla \tilde{v}).\mathbf{p} + \frac{\partial \mathbf{p}}{\partial t} + \mathbf{p}.(\nabla \tilde{v}) \right] = -k \nabla T, \tag{1}$$

For concentration,

$$\mathbf{q} + \lambda_q \left[(\nabla \mathbf{q}).\tilde{v} - (\nabla \tilde{v}).\mathbf{q} + \frac{\partial \mathbf{q}}{\partial t} + \mathbf{q}.(\nabla \tilde{v}) \right] = -D_B \nabla C, \tag{2}$$

Here, heat flux term is represented with the $\mathbf{p}$, whereas mass flux term is represented with the $\mathbf{q}$. Then, the Cattaneo–Christov defined the relaxation times of heat and mass that are represented ads λ_p and λ_q respectively. The above equations also represent the thermal conductivity as k and Brownian diffusion parameter as D_B. The equations represented in above are reduced for the sake of steady and incompressible nanofluid in such a form as follows:

$$\mathbf{p} + \lambda_p \left[\frac{\partial \mathbf{p}}{\partial t} - \mathbf{p} \cdot (\nabla \tilde{v}) + \tilde{v} \cdot (\nabla \mathbf{p}) \right] = -k \nabla T, \tag{3}$$

$$\mathbf{q} + \lambda_q \left[\frac{\partial \mathbf{q}}{\partial t} - \mathbf{q} \cdot (\nabla \tilde{v}) + \tilde{v} \cdot (\nabla \mathbf{q}) \right] = -D_B \nabla C, \tag{4}$$

The Cattaneo–Christov model enables us to derive the following equations (notice, for an instance, Ahmad et al. [35]) together with using of Oberbeck–Boussinesq approximation.

$$\frac{\partial u}{\partial x} + \frac{\partial v}{\partial y} = 0, \tag{5}$$

$$\begin{aligned} u\frac{\partial u}{\partial x} + v\frac{\partial u}{\partial y} - U_s\frac{\partial U_s}{\partial x} - \upsilon\frac{\partial^2 u}{\partial y^2} &= \frac{\pi j_0 M(x) \exp\left(-\frac{\pi}{b}y\right)}{8\rho_f} \\ &+ \frac{\delta_1}{\rho_f}\left(\frac{\partial u}{\partial x}\frac{\partial}{\partial y}\left(\frac{\partial u}{\partial y}\right) + u\frac{\partial}{\partial x}\left(\frac{\partial^2 u}{\partial y^2}\right) - \frac{\partial u}{\partial y}\frac{\partial}{\partial x}\left(\frac{\partial u}{\partial y}\right) + v\frac{\partial^3 u}{\partial y^3}\right) \\ &+ \frac{1}{\rho_f}\left[\rho_f \beta_T (1 - C_\infty)(T - T_\infty) - (C - C_\infty)(\rho_f - \rho_{f\infty})\right] g, \end{aligned} \tag{6}$$

$$\begin{aligned} &u\frac{\partial T}{\partial x} + v\frac{\partial T}{\partial y} - \alpha\frac{\partial^2 T}{\partial y^2} \\ &+\lambda_p \begin{pmatrix} v\frac{\partial v}{\partial y}\frac{\partial T}{\partial y} + u\frac{\partial u}{\partial x}\frac{\partial T}{\partial x} + v\frac{\partial u}{\partial y}\frac{\partial T}{\partial x} \\ +u\frac{\partial v}{\partial x}\frac{\partial T}{\partial y} + u^2\frac{\partial^2 T}{\partial x^2} + v^2\frac{\partial^2 T}{\partial y^2} + 2uv\frac{\partial^2 T}{\partial x \partial y} \end{pmatrix} = \\ &\qquad -\frac{1}{(\rho c)_f}\frac{\partial Q_R}{\partial y} + \tau\left(D_B\left(\frac{\partial T}{\partial y}\frac{\partial C}{\partial y}\right) + \frac{D_T}{T_\infty}\left(\frac{\partial T}{\partial y}\right)^2\right), \end{aligned} \tag{7}$$

$$\begin{aligned} &u\frac{\partial C}{\partial x} + v\frac{\partial C}{\partial y} - D_B\frac{\partial^2 C}{\partial y^2} \\ &+ \lambda_p \begin{pmatrix} v\frac{\partial v}{\partial y}\frac{\partial C}{\partial y} + u\frac{\partial u}{\partial x}\frac{\partial C}{\partial x} + v\frac{\partial u}{\partial y}\frac{\partial C}{\partial x} \\ +u\frac{\partial v}{\partial x}\frac{\partial C}{\partial y} + u^2\frac{\partial^2 C}{\partial x^2} + v^2\frac{\partial^2 C}{\partial y^2} + 2u\,v\frac{\partial^2 C}{\partial x \partial y} \end{pmatrix} \\ &= \frac{D_T}{T_\infty}\left(\frac{\partial^2 T}{\partial y^2}\right) - k * (C - C_\infty), \end{aligned} \tag{8}$$

with

$$\begin{aligned} &u = U_w = 0,\ v = 0,\ -k\frac{\partial T}{\partial y} = -h_f(T - T_f), \\ &\frac{D_T}{T_\infty}\left(\frac{\partial T}{\partial y}\right) = -D_B\frac{\partial C}{\partial y},\ \text{at}\ y = 0, \end{aligned} \tag{9}$$

$$u \to U_s = u_\infty = ax,\ \frac{\partial u}{\partial y} \to 0,\ T \to T_\infty,\ C \to C_\infty,\ \text{as } y \to \infty. \tag{10}$$

Such that, $M(x) = Mx$ is the given magnetization, b is width, j_0 is the density of applied electrodes and magnets, k^* is chemical reaction rate constant, kinematic viscosity is given by υ, dynamic viscosity is given by μ, density is given by ρ_f, thermal diffusivity is given by α, τ is defined as effectively productive heat capacity for the given base fluid and nanoparticles, $(\rho c)_f$ is productive heat capacity of liquid, D_T is the thermophoretic effect, D_B is the Brownian motion, β_T is thermal expansion, and h_f is heat flux coefficient.

Nonlinear radiative heat flux is [39–41]

$$Q_R = -\frac{4\widetilde{\sigma}}{3\widetilde{k}}\frac{\partial T^4}{\partial y} = -\frac{16\widetilde{\sigma}T_\infty^3}{3\widetilde{k}}\frac{\partial T}{\partial y}, \tag{11}$$

here, $\widetilde{\sigma}$ is Stefan–Boltzmann constant, $\tilde{k}$ is mean absorption coefficient. Define

$$v = -\frac{\partial \psi}{\partial x},\ u = \frac{\partial \psi}{\partial y},\ \eta = \sqrt{\frac{a}{\upsilon}}y,\ \psi = x\sqrt{\upsilon a}s(\eta),$$
$$T_\infty = T + \theta(\eta)\left(T_\infty - T_f\right), f(\eta)C_\infty + C_\infty = C. \tag{12}$$

Using Eq. (12) into Eqs. (6)–(10), the velocity, temperature and nanoparticle concentration with boundary conditions are presented as follows:

$$s''' + ss'' - s'^2 + \delta\left(2s's'' - s''^2 - ss^{iv}\right) + \Gamma(\theta - \mathrm{Nr}f) + \mathrm{He}^{-\beta_1\eta} + 1 = 0, \tag{13}$$

$$\left(1 + \frac{4}{3}\mathrm{Rd}\right)\frac{1}{\mathrm{Pr}}\theta'' + s\theta' + \mathrm{Nb}f'\theta' + \mathrm{Nt}\,\theta'^2 - \lambda_1\left(s^2\theta'' + ss'\theta'\right) = 0, \tag{14}$$

$$f'' + \frac{\mathrm{Nt}}{\mathrm{Nb}}\theta'' + \mathrm{Le\ Pr}\,sf' - \mathrm{Pr\ Le}\,\lambda_2\left(ss'f' + s^2f''\right) - \mathrm{Pr\ Le}\,\gamma f = 0, \tag{15}$$

With following BC's

$$s(0) = s'(0) = 0,\ \theta'(0) = B_{it}(\theta(0) - 1),\ f'(0) = -\frac{\mathrm{Nt}}{\mathrm{Nb}}\theta'(0),$$
$$s'(\infty) \to 1,\ s''(\infty) \to 0,\ \theta(\infty) \to 0,\ f(\infty) \to 0, \tag{16}$$

where $\delta = \frac{\delta_1 a}{\mu}$, $\lambda_1 = \lambda_p a$ and $\lambda_2 = \lambda_q a$ are known as fluid parameters, $\beta_1 = \frac{\pi}{b}\sqrt{\frac{\upsilon}{a}}$ is a strictly dimensionless parameter, $\mathrm{Pr} = \frac{\upsilon}{\alpha}$ is Prandtl factor, $\mathrm{Nb} = \frac{\tau D_B C_\infty}{\upsilon}$ Brownian motion parameter, $\mathrm{Nt} = \frac{\tau D_T(T_f - T_\infty)}{\upsilon T_\infty}$ thermophoresis factor, $B_{\mathrm{it}} = \frac{h_f}{k}\sqrt{\frac{\upsilon}{a}}$ is Biot number, $H = \frac{\pi j_0 M_0}{8a^3\rho_f}$ is known as modified Hartman number, $\mathrm{Rd} = \frac{4\widetilde{\sigma}T_\infty^3}{(\rho c)_f\tilde{k}}$ is radiation parameter, $\mathrm{Le} = \frac{\alpha}{D_B}$ is Lewis factor, and $\Gamma = \frac{\mathrm{Gr}}{\mathrm{Re}_x^2}$ is Richardson number known as mixed convection parameter: for the values of $(\Gamma > 0)$ accounts for heated surface, $(\Gamma < 0)$ corresponds to cold surface, and $(\Gamma = 0)$ indicates the forced convection flow, $\mathrm{Gr} = \frac{g\beta_t(1-C_\infty)(T_f - T_\infty)x^3}{\upsilon^2}\frac{\rho_f}{\rho_\infty}$ is Grashof number, chemical reaction $\gamma = \frac{k_0}{a}$ such that $(\gamma > 0)$ allied to destructive chemical reaction and $(\gamma < 0)$ connected to the generative chemical reaction.

The important physical quantities are given by using $Re_x = \frac{x_1 u_\infty}{\upsilon}$:

$$\mathrm{Cf} = \mathrm{Re}_x^{1/2}\mathrm{Cf}_x = s''(0) + 3\delta s'(0)s''(0),$$
$$\mathrm{Nu} = \mathrm{Re}_x^{-1/2}\mathrm{Nu}_x = -\theta'(0). \tag{17}$$

3 Method of Solution

In addition with shooting technique and fourth–fifth-order method of Runge–Kutta–Fehlberg used in the solutions of boundary conditions (16) and nonlinear ordinary differential Eqs. (13)–(15) in the system, differential equations of second order are θ and f and fourth order is s in the system. s, θ and f are reduced in the first step to the first-order differential equations which are as follows:

$$\Psi_1' = \Psi_2, \tag{18}$$

$$\Psi_2' = \Psi_3, \tag{19}$$

$$\Psi_3' = \Psi_4, \tag{20}$$

$$\Psi_4' = \frac{1}{\delta\Psi_1}\left[\Psi_4 + \Psi_1\Psi_3 - \Psi_2^2 + 2\delta\,\Psi_2\Psi_4 - \delta\Psi_3^2 + \Gamma\left(\Psi_5 - \mathrm{Nr}\,\Psi_7\right) + \mathrm{He}^{-\beta_1\eta} + 1\right], \tag{21}$$

$$\Psi_5' = \Psi_6, \tag{22}$$

$$\Psi_6' = -\frac{3}{3 + 4\mathrm{Rd} - 3\lambda_1\Psi_1^2}\left[\mathrm{Pr}\,\Psi_1\Psi_6 + \mathrm{Pr\,Nb}\Psi_6\Psi_8 + \mathrm{Pr\,Nt}\Psi_6^2\right], \tag{23}$$

$$\Psi_7' = \Psi_8, \tag{24}$$

$$\Psi_8' = \frac{1}{1 + \mathrm{Pr\,Le}\lambda_2\Psi_1^2}\left[\mathrm{Pr\,Le}\lambda_2\Psi_1\Psi_2\Psi_8 - \frac{\mathrm{Nt}}{\mathrm{Nb}}\Psi_6' - \mathrm{Pr\,Le}\Psi_1\Psi_8 + \mathrm{Pr\,Le}\gamma\,\Psi_7\right], \tag{25}$$

where $\Psi_1 = s,\ \Psi_2 = s',\ \Psi_3 = s'',\ \Psi_4 = s''',\ \Psi_5 = \theta,\ \Psi_6 = \theta',\ \Psi_7 = f,\ \Psi_8 = f'$ and according to η derivative of the function is denoted by the prime.

Then, the conditions of the corresponding boundary are.

$$\Psi_1 = \Psi_2 = 0,\ \Psi_6 = B_{it}\left(\Psi_5 - 1\right),\ \Psi_8 + \frac{\mathrm{Nt}}{\mathrm{Nb}}\Psi_6 = 0,\ \text{at}\ \eta = 0, \tag{26}$$

$$\Psi_2 \to 1,\ \Psi_3 \to 0,\ \Psi_5 \to 0,\ \Psi_7 \to 0,\ \text{as}\ \eta \to 0. \tag{27}$$

The unknown values of $\Psi_3(0), \Psi_6(0)$ and $\Psi_8(0)$ are calculated by using the technique of shooting. The calculating process of $\Psi_3(0), \Psi_6(0)$ and $\Psi_8(0)$ starts with some parameters guessing. The process of guessing is repeated with η_∞ awaiting of difference of desired accuracy with the repeated values of $\Psi_3(0), \Psi_6(0)$ and $\Psi_8(0)$. At $\eta = 10$, the calculated values of s', θ and f are compared with predefined boundary conditions and for better approximation, estimated values are adjusted to $s''(0), \theta'(0)$ and $f'(0)$. There is an occurrence of small changes in temperature and velocity in the finite value of η and one value must be taken from the infinity condition as large. Far-field boundary conditions are achieved by considering the bulk computations with value at $\eta_\infty = 8$ or 10 where all parameters are to be considered.

Runge–Kutta–Fehlberg fourth–fifth-order (RKF-45) method is used in the integration process after the finite value for η_∞ fixing. If step size h is proper then it is used in the integration process to find the solution through this method. Two different approximations are considered and comparison happens between them in the first step. This process of approximation is carried out until the two results are close to each other. If this state obtained then the approximation is accepted if not then this process is continued with reduced step size. Step size $\Delta\eta = 0.001, \eta_\infty = 8$ or 10 are taken for the current problem, and eight places are considered for accuracy.

Table 1 The results validation RKFM for s$f''(0)$, with those of the literature when $P = 5$, $\beta_1 = 0.5$, Nt = .5, Nr = 0.1, Nb = 0.5, Le = 0.1, $B_{\mathrm{it}} = 50$ and $\delta = \lambda_1 = \mathrm{Rd} = \mathrm{Kr} = \lambda_2 = 0$

H	Γ	Ahmad et al. [35]		Present outcomes
		RKM	bvp4c	RKF-45
		$f''(0)$	$f''(0)$	$f''(0)$
0.0	0.5	1.4294038	1.4294037	1.42940372
0.5		1.7243537	1.7243587	1.72435366
1.0		2.0099196	2.0099297	2.00991955
1.5		2.2874751	2.2874603	2.28746020
0.5	0	1.5394682	1.5394732	1.53946801
	1	1.9023442	1.9023488	1.90234428
	2	2.2416224	2.2416273	2.24162262
	3	2.5631502	2.5631452	2.56314556
	4	2.8705968	2.8706019	2.87059730

Table 2 The results validation of RKFM for $-\theta'(0)$, with those of the literature when Pr = 5, $\beta_1 = 0.5$, Nt = 0.5, Nr = 0.1, Nb = 0.5, Le = 0.1, $B_{\mathrm{it}} = 50$ and $\delta = \lambda_1 = \mathrm{Rd} = \mathrm{Kr} = \lambda_2 = 0$

H	d_1	B_{it}	Ahmad et al. [35]		Present outcome
			RKM	bvp4c	RKF-45
			$-\theta'(0)$	$-\theta'(0)$	$-\theta'(0)$
0.0	0.2	5	0.52262732	0.52262707	0.52262702
0.5			0.55588512	0.55592229	0.55588488
1.0			0.58383262	0.58389767	0.58383242
1.5			0.60801213	0.60809909	0.60801194
0.5	0.1	5	0.56029900	0.56030037	0.56017544
	0.2		0.55592167	0.55592274	0.55588488
	0.3		0.55232480	0.55232517	0.55231292
	0.4		0.54930674	0.54930711	0.54930274
	0.2	0.0	0.00000000	0.00000000	0.00000000
		0.5	0.27715283	0.27715312	0.27714344
		1.0	0.38397307	0.38397360	0.38395525
		1.5	0.44069949	0.44070018	0.44067615

Present results are compared with the previously published results Ahmad et al. [35], for Nusselt number and local skin friction for several values of the Hartman and Richardson numbers as a special case and shown in Table 1 and 2. An excellent agreement is achieved and confidence in the present RKF 45 solutions is, therefore, justifiable high.

4 Results and Discussion

Second-grade nanofluid generated by the Riga plate subject to thermal radiation and chemical reaction in the convective theoretical investigation is performed. By using the Runge–Kutta–Fehlberg fourth–fifth-order method, the given differential equations are numerically solved with the present formulation. In order to study the behaviour of temperature, volume fraction profile of nanoparticle for Hartman number (H), velocity distribution, Richardson number (Γ), fluid relaxation parameters (λ_1, λ_2), radiation parameter (Rd), Biot number (B_{it}), thermophoresis factor (Nt) and Brownian motion parameter (Nb), graphs are plotted and behind the graphs physical reasons are discussed. The values $\mathrm{Pr} = 7, B_{\mathrm{it}} = 2, \beta_1 = 0.2, \mathrm{Nt} = 0.1, \lambda_1 = 10^{-3}, \mathrm{Nb} = 0.1, \lambda_2 = 10^{-3}$, Le = 0.1, $\gamma = 0.1$, $H = 1, \delta = 0.5$, and $\Gamma = 0.1$ are taken as default parameters; otherwise, graphical and tabular description is made.

The flow pattern produced for Hartman number in Figs. 2 and 3. It is observed that streamlines are closed to the stagnation point for higher values of Hartman number. On liquid movement, impact of number of fluid parameters is analysed

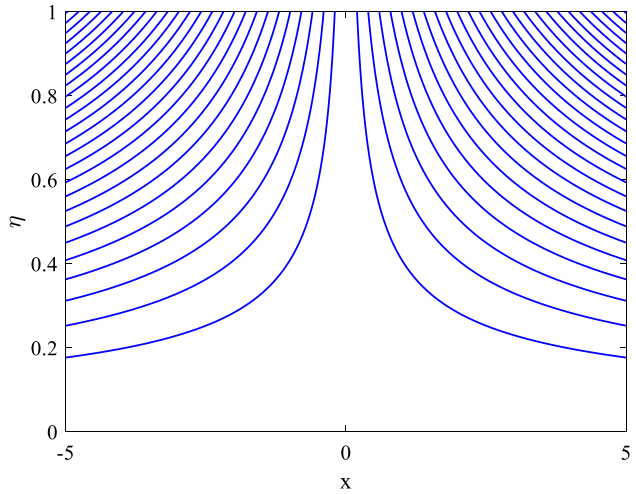

Fig. 2 Streamlines for $H = 1$

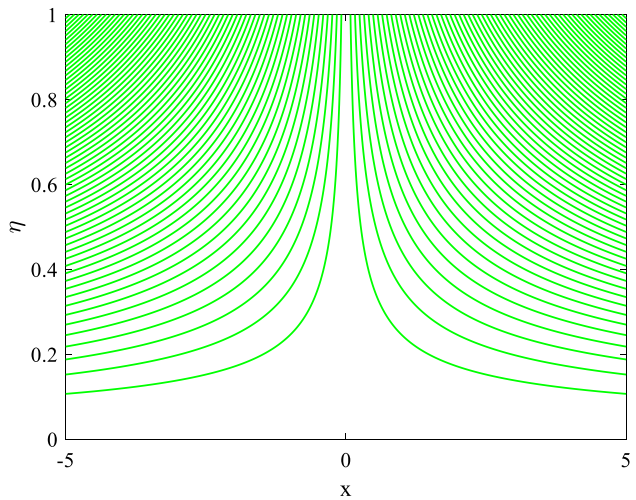

Fig. 3 Streamlines for $H = 10$

in Figs. 4 and 5. With higher numerical values of δ fluid velocity decreased, the second-grade nanofluid parameter δ influence is sketched graphically in Fig. 4. The obtained results are very close to Riga plate surface rather than the away from surface. Viscosity of the fluid and fluid parameter of second-grade augmented values have the direct relation between them.

Figure 4 also influences display of Hartman number (modified) (H) on fluid movement. To enhance the momentum flow in fluid flow along the x_1-axis the parallel direction, Riga pattern actives the Lorentz force effectively in physical and increases the thickness of connected boundary layer. In the flow profile, against the augmented values a mixed nature is noticed and in Fig. 5 these convection parameters are presented. Velocity profile is increased when

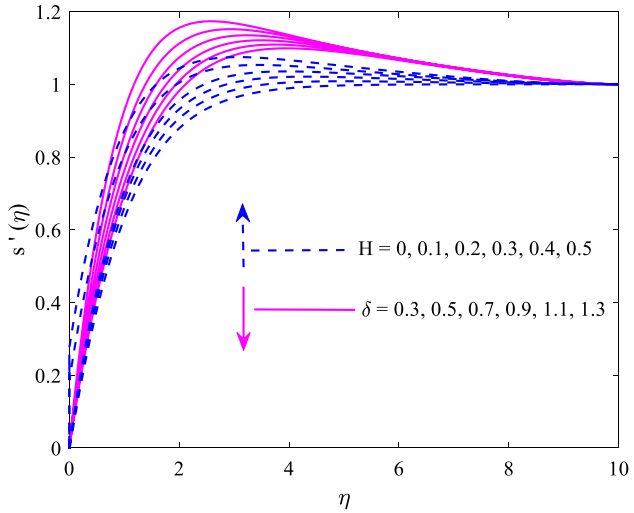

Fig. 4 Variation regarding H and δ over velocity

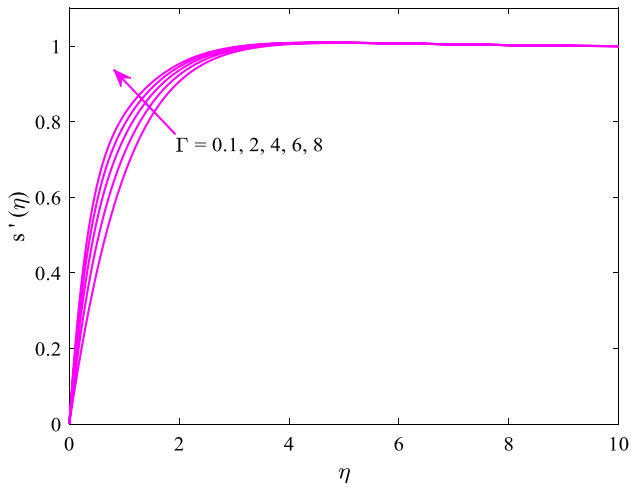

Fig. 5 Variation regarding Γ over velocity

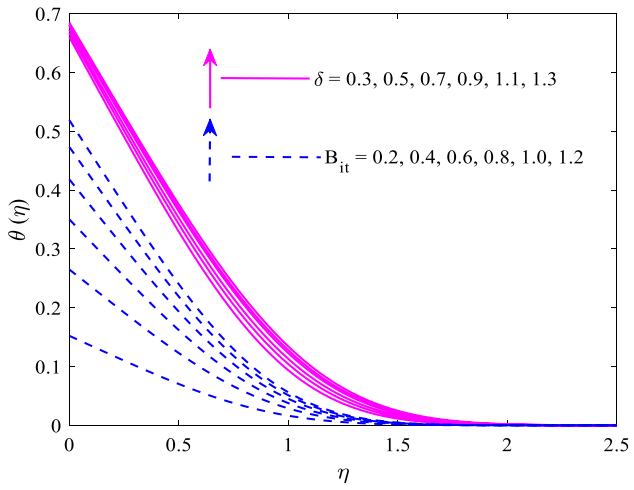

Fig. 6 Variation regarding δ and B_{it} over temperature

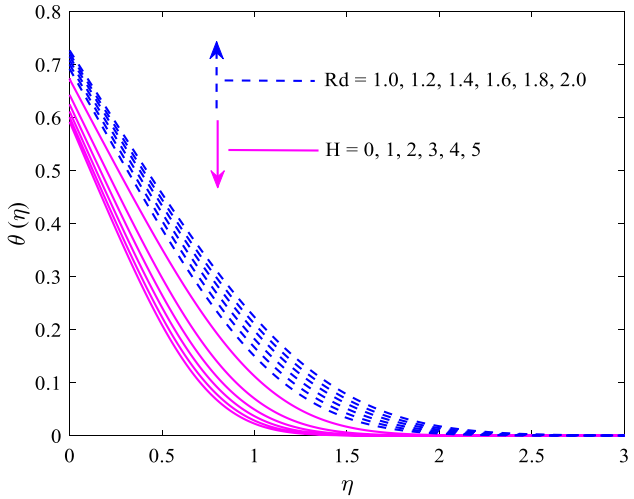

Fig. 7 Variation regarding Rd and H over temperature

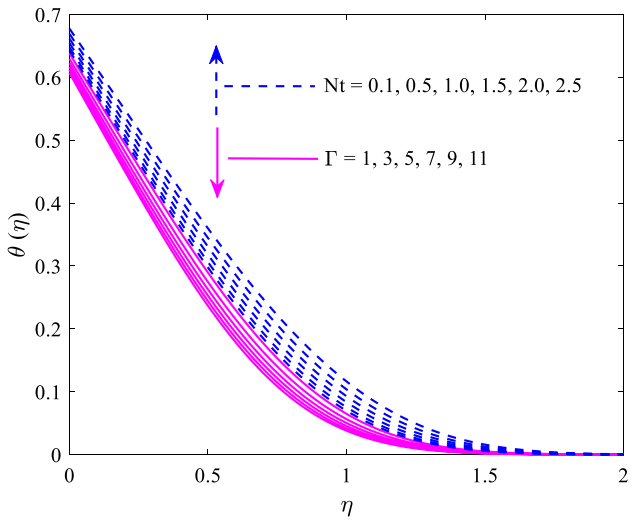

Fig. 8 Variation regarding Nt and Γ over temperature

on the fluid high intensive buoyancy forces are augmented in Γ. For upward flow close to the Riga surface, supportive pressure gradient is supposed by the larger Γ physically and enhances the s'. The point at which the behaviour is changed and Lorentz force is dominated by velocity of free stream at large values of Γ.

Thermal distribution versus different fluid parameters graphical results are plotted from Figs. 6, 7, 8 and 9. The nanofluid parameter δ of second grade and the variation in the Biot factor B_{it} versus temperature distribution behaviour are plotted in Fig. 6. The Biot factor larger values are noticed in the thermal profile elevation. Because of Biot number, a major strength is evolved. Iso-flux situation is achieved for Biot number which is close to 0, whereas isothermal state is achieved for more values of Biot number. In Fig. 6 fluid

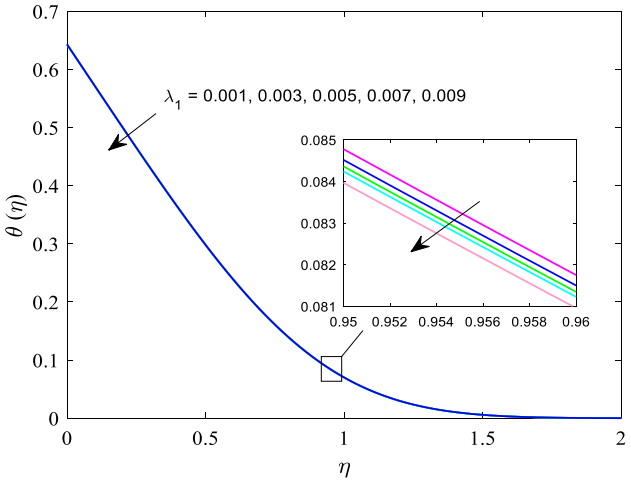

Fig. 9 Variation regarding λ_1 over temperature

under consideration, second-grade nanofluid factor impacts on fluid thermal state are plotted. Heat transfer enhancement is achieved by noticing the elevated trend in the wall temperature.

The influence of the temperature field on modified radiation factor (Rd) and Hartman factor (H) is plotted in Fig. 7. Between H and θ, an inverse relationship is noticed. Hartman number modified values; in temperature field certain decline is noticed. Thermal profile is reduced by the fluid flow which is assisted by the induced Lorentz force. The impact of thermal radiation factor is also plotted in Fig. 7, in which the temperature is enhanced by the radiation factor Rd and its influences are indicated. Temperature is increased with the help of radiation factor Rd which gives the heat to equivalent fluid.

The effect of thermophoresis factor and mixed convection in thermal state is illustrated in Fig. 8. For stronger thermophoresis, temperature field enhancement is noticed. Here, the thermophoresis is a method of moving from hot region hot particles to cold region and then rises the temperature consequently. In the energy equation, mixed convection parameter Γ is not appeared directly, but small temperature profile is anticipated. Γ is incremented with decrement in temperature which is depicted in Fig. 8. The thermal profile versus relaxation time parameter λ_1 display is illustrated in Fig. 9. Furthermore, thermal relaxation parameter λ_1 is increased in physical interpretation that requires more heat for transmitting heat to its corresponding material particles (which are non-conducting type), for the temperature profile reduction as a fundamental.

Figures 10, 11, 12 and 13 are depicted by the changes noted in concentration fluid distribution according to the different parameters of fluid elevated values. In particular, Fig. 10, second-grade nanofluid parameter versus a mixed behaviour of the concentration distribution is observed.

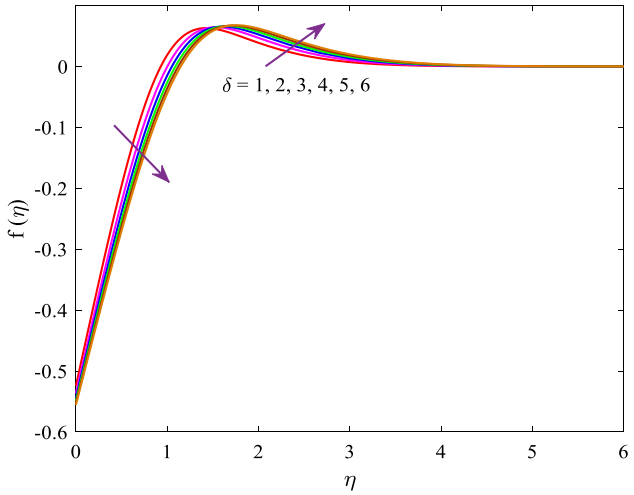

Fig. 10 Variation regarding δ over concentration

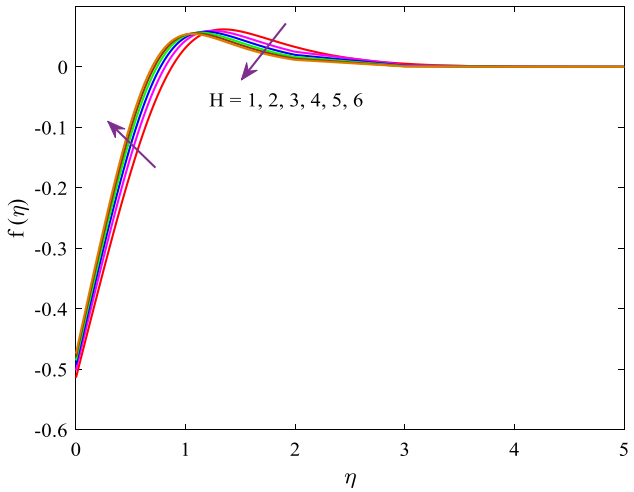

Fig. 11 Variation regarding H over concentration

Reduction is noticed at the closer to surface and increment is noticed at far away from surface. Figure 11 describes the behaviour of nanoparticle concentration (f) for Hartman modified factor. For large H, nanoparticles concentration is improved when velocity field is opposite. Riga plate generates Lorentz forces and variation is depended on these for ces.

The influences of thermophoresis on Brownian diffusion are illustrated in Fig. 12. Figure 12 witnesses that Brownian motion produces resistance in concentration of nanoparticle. Profile of nanoparticle concentration and thickness of boundary layer is reduced by the collision of particles enhancement with the Brownian motion parameter increases. Figure 12 also gives thermophoretic force augmented values impact on the nanoparticles concentration.

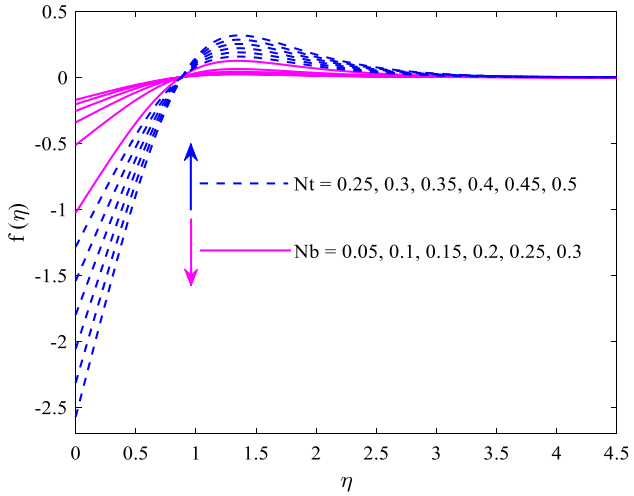

Fig. 12 Variation regarding Nt and Nb over concentration

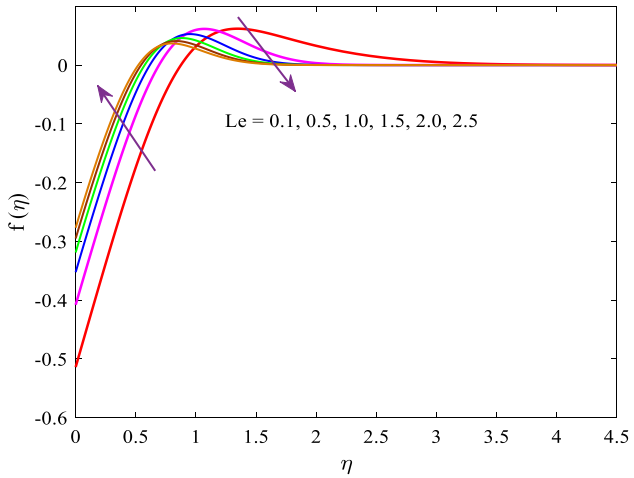

Fig. 13 Variation regarding Le over concentration

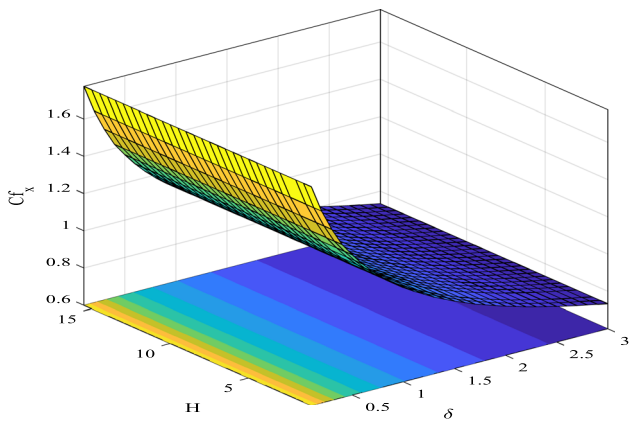

Fig. 14 Variation regarding H and δ over skin friction

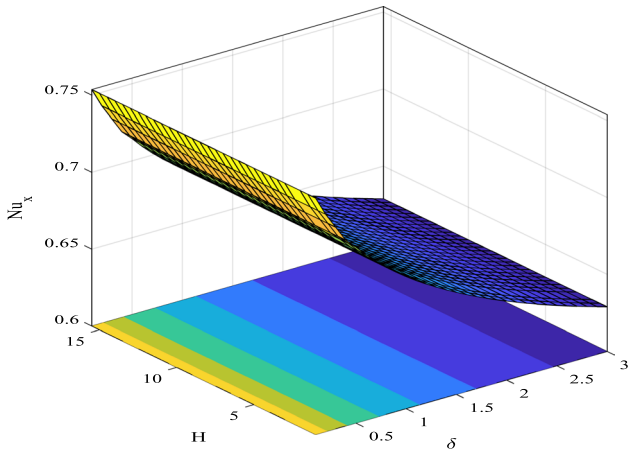

Fig. 15 Variation regarding H and δ over heat transfer rate

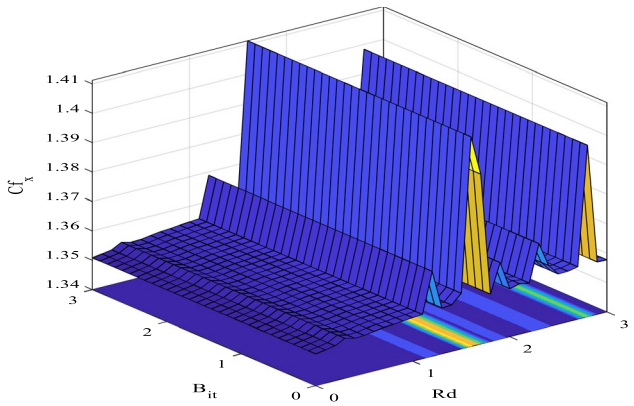

Fig. 16 Variation regarding B_{it} and Rd over skin friction

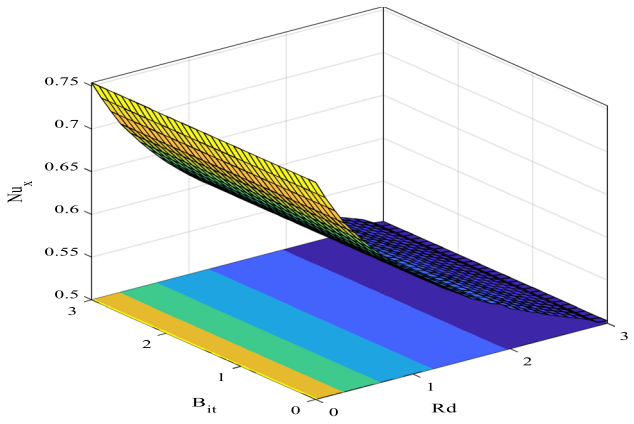

Fig. 17 Variation regarding B_{it} and Rd over heat transfer rate

Nanoparticles gaps are created by the fluid in-predictive movement which is enhanced by the thermophoretic stronger forces. Figure 13 explains the behaviour of Lewis number Le on concentration distribution. It is seen that the distribution concentration is a diminishing function of Le. Justification of such a decreasing behaviour is elaborated as Le and Lewis number leading values concentrated as low by mass diffusivity with reverse relations.

Figures 14, 15, 16 and 17 give the 3D graphical illustrations of Nusselt factor (heat flux) and skin friction (wall drag force) for several fluid parameters elevated values. Clearly, the drag force intensifies for second-grade parameter augmented nature and stronger Lorentz forces. Mixing behaviour is observed in drag force with the impact of radiation parameter. The heat flux reduces for increasing values of nanofluid parameter second-grade and radiation factor, but the larger Lorentz force and Biot number result in increment in heat flux.

5 Concluding Remarks

The main aim of this work is to utilize the Cattaneo–Christov heat flux and generalized Fick's theories with the intention of study the mass and heat transportation in the modified nanofluid second-grade over a Riga plate with thermal radiation additional features and chemical reaction. Moreover, the assumptions of convective heating for temperature distribution and new zero mass flux condition for distribution concentration are forced for the recognized flow situation. Through appropriate adjusted transformations, ordinary nonlinear equations are obtained from the proposed flow. These equations are solved by using the method of Runge–Kutta–Fehlberg fourth–fifth order (RKF-45) to obtain numerical solution. The present discussed analysis gives the following results:

1. Augmented trend for incremental values of modified factor of Hartman showed by the associated boundary layer and velocity field.
2. Temperature distribution and fluid horizontal movement reduction are confirmed by the second-grade parameter.
3. Temperature field rejection and thermal profile are influenced by the modified Hartman factor. Cattaneo–Christov model is dominated by the Fourier's model trend which is confirmed by the thermal boundary layer.
4. Thermal profile and temperature field are significantly influenced with radiation factor.
5. For Biot number augmented values, in the thermal profile noticed an enhancement, the temperature for larger Biot number is raised with convective heating results of significant strength. Iso-flux situation is achieved for Biot number which is close to 0, whereas isothermal state is achieved for more values of Biot number for the temperature field.

6. Dimensionless concentration is negative in the vicinity if the plate illustrating that nanoparticle concentration at the wall is smaller than that at the ambient.
7. Nanofluid second-grade parameter and modified Hartman number larger values are amplified by the skin friction.
8. The heat flux enhanced for elevated values of modified Hartman number and Biot number; it reduces for second-grade nanofluid parameter and radiation factor.
9. From the special cases of previously discussed, the present work is extracted and the obtained results are compared with the existing results [35]. A better agreement between the already published work and present is found.

The present model has considered non-Newtonian nanofluids. Further investigation will address non-Newtonian bioconvection nanofluid in porous media considering slip mechanism and will be reported in due course.

Acknowledgements The authors are highly obliged and thankful to unanimous reviewers for their valuable comments on the paper.

References

1. Choi, S.U.S.: Enhancing thermal conductivity of fluids with nanoparticles. Proc. ASME Int. Mech. Eng. Cong Exp. **66**, 99–105 (1995)
2. Beiki, H.: Developing convective mass transfer of nanofluids in fully developed flow regimes in a circular tube: modeling using fuzzy inference system and ANFIS. Int. J. Heat Mass Transf. **173**, 121285 (2021)
3. Buongiorno, J.: Convective transport in nanofluids. J. Heat Transf. **128**(3), 240–250 (2006)
4. Kuznetsov, A.V.; Nield, D.A.: Natural convective boundary-layer flow of a nanofluid past a vertical plate. Int. J. Therm. Sci. **49**, 243–247 (2010)
5. Daniel, Y.S.; Aziz, Z.A.; Ismail, Z.; Bahar, A.: Unsteady EMHD dual stratified flow of nanofluid with slips impacts. Alex. Eng. J. **59**(1), 177–189 (2020)
6. Gangadhar, K.; Kannan, T.; Jayalakshmi, P.: Magnetohydrodynamic micropolar nanofluid past a permeable stretching/shrinking sheet with Newtonian heating. J Braz. Soc. Mech. Sci. Eng. **39**, 4379–4391 (2017)
7. Hashimoto, S.; Yano, K.; Hirota, Y.; Uchiyama, H.; Tsutsui, S.: Analysis of enhancement mechanism for thermal conductivity if nanofluids by inelastic X-ray scattering. Int. J. Heat Mass Transf. **173**, 121245 (2021)
8. Kanti, P.K.; Sharma, K.V.; Said, Z.; Gupta, M.: Experimental investigation on thermo-hydraulic performance of water-based fly ash-Cu hybrid nanofluid flow in a pipe at various inlet fluid temperatures. Int. Commun. Heat Mass. **124**, 105238 (2021)
9. Vinoth, R.; Sachuthananthan, B.: Flow and heat transfer behavior of hybrid nanofluid through microchannel with two different channels. Int. Commun. Heat Mas **123**, 105194 (2021)
10. Kanti, P.; Sharma, K.V.; Said, Z.; Kesti, V.: Entropy generation and friction factor of fly ash nanofluids flowing in a horizontal tube: experimental and numerical study. Int. J. Therm. Sci. **166**, 106972 (2021)
11. Saleh, B.; Syam Sundar, L.: Experimental study on heat transfer, friction factor, entropy and exergy efficiency analyses of a corrugated plate heat exchanger using Ni/water nanofluids. Int. J. Therm. Sci. **165**, 106935 (2021)
12. Sáchica, D.; Treviño, C.; Martínez-Suástegui, L.: Numerical study of magnetohydrodynamic mixed convection and entropy generation of Al_2O_3-water nanofluid in a channel with two facing cavities with discrete heating. Int. J. Heat Fluid Flow **86**, 108713 (2020)
13. Zakaria, I.A.; Mohamed, W.A.N.W.; Zailan, M.B.; Azmi, W.H.: Experimental analysis of SiO_2-Distilled water nanofluids in a polymer electrolyte membrane fuel cell parallel channel cooling plate. Int. J. Hydrog. Energy **44**(47), 25850–25862 (2019)
14. Ya Rudyak, V.; Minakov, A.V.; Pryazhnikov, M.I.: Preparation, characterization, and viscosity studding the single-walled carbon nanotube nanofluids. J. Mol. Liq. **329**, 115517 (2021)
15. Shit, S.P.; Pal, S.; Ghosh, N.K.; Sau, K.: Thermophysical properties of graphene and hexagonal boron nitride nanofluids: a comparative study by molecular dynamics. J. Mol. Struct. **1239**, 130525 (2021)
16. Bahiraei, M.; Mazaheri, N.: A comprehensive analysis for second law attributes of spiral heat exchanger operating with nanofluid using two-phase mixture model: exergy destruction minimization attitude. Adv. Powder Technol. **32**(1), 211–224 (2021)
17. Ji, W.; Yang, L.; Chen, Z.; Mao, M.; Huang, J.: Experimental studies and ANN predictions on the thermal properties of TiO_2-Ag hybrid nanofluids: consideration of temperature, particle loading, ultrasonication and storage time. Powder Technol. **388**, 212–232 (2021)
18. Tanveer, A.; Malik, M.Y.: Slip and porosity effects on peristalsis of MHD Ree-Eyring nanofluid in curved geometry. Ain Shams Eng. J. **12**(1), 955–968 (2021)
19. Rafiq, M.; Shafique, M.; Azam, A.; Ateeq, M.: Transformer oil-based nanofluid: the application of nanomaterials on thermal, electrical and physicochemical properties of liquid insulation—a review. Ain Shams Eng. J. **12**(1), 555–576 (2021)
20. Rivlin, R.S.; Ericksen, J.L.: Stress deformation relations for isotropic materials. J. Ration Mech. Anal. **4**, 323–425 (1955)
21. Imtiaz, M.; Mabood, F.; Hayat, T.; Alsaedi, A.: Homogeneous-heterogeneous reactions in MHD radiative flow of second grade fluid due to a curved stretching surface. Int. J. Heat Mass Transf. **145**, 118781 (2019)
22. Adeniyan, A.; Mabood, F.; Okoya, S.S.: Effect of heat radiating and generating second-grade mixed convection flow over a vertical slender cylinder with variable physical properties. Int. Commun. Heat Mass **121**, 105110 (2021)
23. Waqas, H.; Khan, S.U.; Hassan, M.; Bhatti, M.M.; Imran, M.: Analysis on the bioconvection flow of modified second-grade nanofluid containing gyrotactic microorganisms and nanoparticles. J. Mol. Liq. **291**, 111231 (2019)
24. Hayat, T.; Aziz, A.; Muhammad, T.; Alsaedi, A.; Mustafa, M.: On magnetohydrodynamic flow of second grade nanofluid over a convectively heated nonlinear stretching surface. Adv. Powder Technol. **27**(5), 1992–2004 (2016)
25. Haq, S.U.; Shah, S.I.A.; Jan, S.U.; Khan, I.: MHD flow of generalized second grade fluid with modified Darcy's law and exponential heating using fractional Caputo-Fabrizio derivatives. Alex. Eng. J. **60**(4), 3845–3854 (2021)
26. Veera Krishna, M.; Ameer Ahamad, N.; Chamkha, A.J.: Hall and ion slip impacts on unsteady MHD convective rotating flow of heat generating/absorbing second grade fluid. Alex. Eng. J. **60**(1), 845–858 (2021)
27. Mallawi, F.O.M.; Bhuvaneswari, M.; Sivasankaran, S.; Eswaramoorthi, S.: Impact of double: stratification on convective flow of a non-Newtonian liquid in a Riga plate with Cattaneo-Christov

double-flux and thermal radiation. Ain Shams Eng. J. **12**(1), 969–981 (2021)
28. Gailitis, A.; Lielausis, O.: On a possibility to reduce the hydrodynamic resistance of a plate in an electrolyte. Appl Magnetohydrodyn. **12**, 143–146 (1961)
29. Avilov, V.V.: Electric and magnetic fields for the Riga plate. Technical Report, FRZ, Rossendorf (1998)
30. Tsinober, A.B.; Shtern, A.G.: Possibility of increasing the flow stability in a boundary layer by means of crossed electric and magnetic fields. Magnetohydrodynamics **3**, 103–105 (1967)
31. Grinberg, E.: On determination of properties of some potential fields. Appl. Magnetohydrodyn. **12**, 147–154 (1961)
32. Pantokratoras, A.; Magyari, E.: EMHD free-convection boundary-layer flow from a Riga-plate. J. Eng. Math. **64**, 303–315 (2009)
33. Ahmad, A.; Asghar, S.; Afzal, S.: Flow of nanofluid past a Riga plate. J. Magn. Magn. Mater. **402**, 44–48 (2016)
34. Ayub, M.; Abbas, T.; Bhatti, M.M.: Inspiration of slip effects on electromagnetohydrodynamics (EMHD) nanofluid flow through a horizontal Riga plate. Eur. Phys. J. Plus **131**, 1–9 (2016)
35. Ahmad, R.; Mustafa, M.; Turkyilmazoglu, M.: Buoyancy effects on nanofluid flow past a convectively heated vertical Riga plate: a numerical study. Int. J. Heat Mass Transf. **111**, 827–835 (2017)
36. Liu, Y.; Jian, Y.; Tan, W.: Entropy generation of electromagnetohydrodynamic (EMHD) flow in a curved rectangular microchannel. Int. J. Heat Mass Transf. **127**, 901–913 (2018)
37. Zainal, N.A.; Nazar, R.; Naganthran, K.; Pop, I.: Unsteady EMHD stagnation point flow over a stretching/shrinking sheet in a hybrid Al_2O_3-Cu/H_2O nanofluid. Int. Commun. Heat Mass **123**, 105205 (2021)
38. Bilal, M.: Micropolar flow of EMHD nanofluid with nonlinear thermal radiation and slip effects. Alex. Eng. J. **59**(2), 965–976 (2020)
39. Abbas, T.; Ayub, M.; Bhatti, M.M.; Rashidi, M.M.; Ali, M.E.S.: Entropy generation on nanofluid flow through a horizontal Riga plate. Entropy **18**, 223 (2016)
40. Bhatti, M.M.; Abbas, T.; Rashidi, M.M.: Effects of thermal radiation and electromagnetohydrodynamic on viscous nanofluid through a Riga plate. Multidiscip Model Mater Struct. **12**(4), 605–618 (2016)
41. Abbas, T.; Hayat, T.; Ayub, M.; Bhatti, M.M.; Alsaedi, A.: Electromagnetohydrodynamic nanofluid flow past a porous Riga plate containing gyrotactic microorganism. Neural. Comput. Appl. **31**, 1905–1913 (2019)
42. Rasool, G.; Wakif, A.: Numerical spectral examination of EMHD mixed convection flow of second-grade nanofluid towards a vertical Riga plate used an advanced version of the revised Buongiorno's nanofluid model. J. Therm. Anal. Calorim. **143**, 2379–2393 (2021)